Stress Testing of Chip Aluminum Polymer Capacitors

Alexander Teverovsky

Jacobs Technology Inc.
NASA/GSFC c.562, 8800 Greenbelt Rd. Greenbelt, MD 20771, USA
Alexander.A.Teverovsky@nasa.gov

ABSTRACT

Layered aluminum polymer capacitors (APC) may be viable replacements to current chip tantalum capacitors due to their lower ESR, weight, and smaller size. So far, there is a lack of information regarding the reliability of these parts. Available technical literature is mostly related to the effect on humidity. Although APCs have a limited moisture resistance, it may be contained to the level sufficient for space applications. In this work, seven types of commercial APCs manufactured by four vendors and rated to voltages from 6.3 to 35 V were used to evaluate reliability of the parts under environmental stresses and highly accelerated life tests. Characteristics of the parts, including breakdown voltages, the level of anomalous charging currents (ACC), capacitance, DF, ESR and leakage currents were measured in the process of storage at high-temperatures (from 100 to 150 °C) and high humidity at 85 °C. Monitored highly accelerated life tests have been carried out at temperatures of 85 °C and 125 °C and voltages varying from 1.2 to 1.9 times the rated voltage. Degradation processes and reliability of APCs have been analyzed and compared to polymer tantalum capacitors.

I. INTRODUCTION

Aluminum electrolytic capacitors with conductive polymer cathodes appeared on the market at the turn of this century, first in cylinder aluminum cases that employed wound sheets of oxidized aluminum foil. The design of these parts was similar to wet electrolytic capacitors that also used anodized rolled aluminum foils. A replacement of wet electrolyte with conductive polymers allowed for a substantial reduction of the equivalent series resistance (ESR) and eliminated one of its most significant reliability problem – evaporation of electrolyte. Chip aluminum polymer capacitors (APC) with stacked oxidized aluminum plates encapsulated in molded cases and capable for surface mount assembly were introduced by KEMET and CDE in 2001 [1, 2]. Currently (2023), Murata manufactures 21 types of ECAS series of APCs in case size 7343 and thickness from 1.4 to 2.8 mm. Parts have capacitances from 15 to 470 μF, voltage ratings from 2 to 25 V, and ESR from 4.5 to 40 mohm. The parts have operating temperature range from -40 °C to 105 °C [3].

Presently, most APCs are manufactured in cylinder cases, but there is an increasing production trend of chip designs by Kemet, CDE, Panasonic, Murata, Wurth Elektronik, AVX, and others. Chips are typically rated to low voltages, below 35 V, with the largest group (~71%) rated between 2 and 4 V, and only ~4% are rated between 20 and 35 V. However, development of new conductive PEDOT:PSS polymers with special additives allows for a substantial increase of operating voltages up to 450 V [4, 5].

The majority of APCs compliant with AEC-Q200 requirements have cylinder case designs and there are only a few types of capacitors produced for automotive industry. Although most chip APCs are manufactured for general purposes and have an operating temperature range from -55 to +105 °C, some types of capacitors are rated to 135 °C [6]. Recently, KEMET introduced A798 series of APCs capable to operate at 125 °C for 3000 hours and withstand 85 °C, 85% RH at rated voltages for 1000 hours [7]. Newly developed Clevios K conductive polymer dispersion in aluminum radial capacitors allowed for achieving lifetimes over 1000 hours at 150 °C [8].

The expected lifetime of liquid aluminum electrolytic capacitors is assumed to double when temperature is reduced by 10 °C, $L \sim 2^{\Delta T/10}$, which corresponds to an activation energy of ~ 0.68 eV. According to Wurth Elektronik, the life of chip APCs increases tenfold when the temperature is reduced by 20 °C, $L \sim 10^{\Delta T/20}$ [9]. This corresponds to a much higher activation energy of ~1.7 eV. At these conditions, 2000 hours life testing at 125 °C would be equivalent to 228 years at operating temperature of 65 °C.

Based on Panasonic reliability test results, the failure rate for SP- series of capacitors is below 8.2 FIT at 105 °C and rated voltage. However, the estimated market failure rate is less than 0.13 FIT at a confidence level of 60% [10]. Leakage

currents of APCs may increase after reflow soldering, under no-load conditions at high temperatures, or in high temperature and high humidity environments. However, in most cases, SP capacitors reduce leakage currents due to self-recovery actions when voltage is applied.

The failure rate for ECAS type APCs manufactured by Murata estimated from the results of returned failed products (customer's incoming inspection, in-process, field failures, etc.) is below 0.5 FIT [3]. The expected lifetime is calculated by the power law, $L \sim 2^{\Delta T/\theta}$; however, parameters of this equation are not disclosed because they vary depending on the type of product.

According to CDE [2], the wear-out (WO) mechanism of APCs' failure is due to a steady increase of ESR caused by the presence of moisture entrapped at the oxide/conductive polymer interface during manufacturing. The sensitivity to moisture was reduced substantially with a new design of ESRH capacitors that can operate at 125 °C and have expected life of more than 10 years in typical, hot running, DC-DC modules. The expected life equation is presented in a form: $L = A \times exp\left[\frac{E_a}{k}\left(\frac{1}{T} - 0.00279\right)\right] \times exp\left[C\left(\frac{1}{RH} - \frac{1}{90}\right)\right]$, where A = 1606 hr, E_a = 0.94 eV, C = 550, T is the temperature in K, and RH is the relative humidity in %.

Reliability of plastic encapsulated APCs with PEDOT conductive polymers in humid environments was studied by CALCE researchers at UMD [11, 12]. The observed dominant failure modes were an increase of leakage current, decrease of capacitance, and increase of ESR. The leakage current failures were due to iron particles in the dielectric aluminum oxide layer that provided paths for the current leakage. The iron particles originated from the iron salt used in the manufacturing process during cathode formation. Based on results of testing at rated voltages in humidity chambers at 85% RH and temperatures of 85 °C and 110 °C, the activation energy of failures caused by capacitance degradation was ~ 0.43 eV. The characteristic life during testing at high humidity differs more than three times (from 550 to 1190 hours) for capacitors from different manufacturers.

Initial characterization of APCs by the NASA Electronic Parts and Packaging (NEPP) program was carried out by D. Liu in 2009 [13] using capacitors manufactured by 5 vendors and rated from 2 to 12 V. All parts had a footprint of EIA 7343. Results of testing showed that 12 thermal vacuum cycles at 10^{-4} Torr between -44 and +105 °C did not significantly change the parts' characteristics. Chip capacitors with laminated structure exhibited the best performance by having lower ESR and higher breakdown voltages compared to cylinder case capacitors with rolled foil.

Considering the progress in design and materials used in manufacturing of chip APCs and the lack of reliability data, there is a need for the performance evaluation of capacitors under stress conditions similar to the quality assessments used for polymer tantalum capacitors (PTC) intended for space applications [14]. In this work, seven types of APCs from four vendors were tested in the process of long-term storage at high temperatures, high humidity, and operation at high temperatures and voltages (monitored highly accelerated life testing, HALT). Degradation processes and acceleration factors for environmental stresses and HALT are discussed and compared to the data for PTCs.

II. EXPERIMENT

Data sheet characteristics of APCs used in this study are shown in Table II.1. The parts were manufactured by four vendors with the same footprint, 7.3×4.3 mm, and thickness of the case (H) that varied from 1.9 to 2.8 mm.

Table II.1. Specified characteristics of the parts used in this study.

Group	Mfr.	C, µF	VR, V	ESR, mohm	DF, %	DCL, µA	T_max, °C	H, mm
1	A	120	6.3	9	6	75	105	1.9
2	B	180	6.3	10	6	45	125	2.8
3	C	150	6.3	15	6	94.5	105	1.9
4	D	100	6.3	15	6	63	105	1.9
5	B	33	10	18	6	13	125	2
6	B	15	25	40	6	15	125	2
7	B	15	35	40	6	53	125	2.8

Capacitance and dissipation factor (DF) were measured at 120 Hz, and ESR at 100 kHz. Different manufacturers are specifying measurements of DC leakage currents (DCL) after 2 to 5 min of electrification. In this work, leakage currents were monitored over time and to reduce the effect of absorption currents, DCL measurements were taken after 1000 sec of electrification. These conditions characterize better operational leakage currents that are typically at least two orders

of magnitude below the specified values. Breakdown voltages (VBR) were measured similar to tantalum polymer capacitors by using a constant currents stress (CCS) test [15], and the level of anomalous charging currents (ACC) was characterized using the power surge testing method [16].

III. HIGH TEMPERATURE STORAGE

High temperature storage (HTS) was carried out in temperature chambers set to 100, 125, and 150 °C using 5 samples for each temperature condition. All part types shown in Table II.1 have been tested for up to 4000 hours, and examples of degradation of AC characteristics in the process of storage for two types of capacitors (180 µF, 6.3 V and 15 µF, 35 V) are shown in Fig. III.1. The rate of degradation increased substantially with temperature and although none of the parts could endure 1000 hours at 150 °C, degradation in all groups was within the acceptable limits after 1000 hours at 125 °C and 6 out of 7 groups passed 4000 hours at 100 °C.

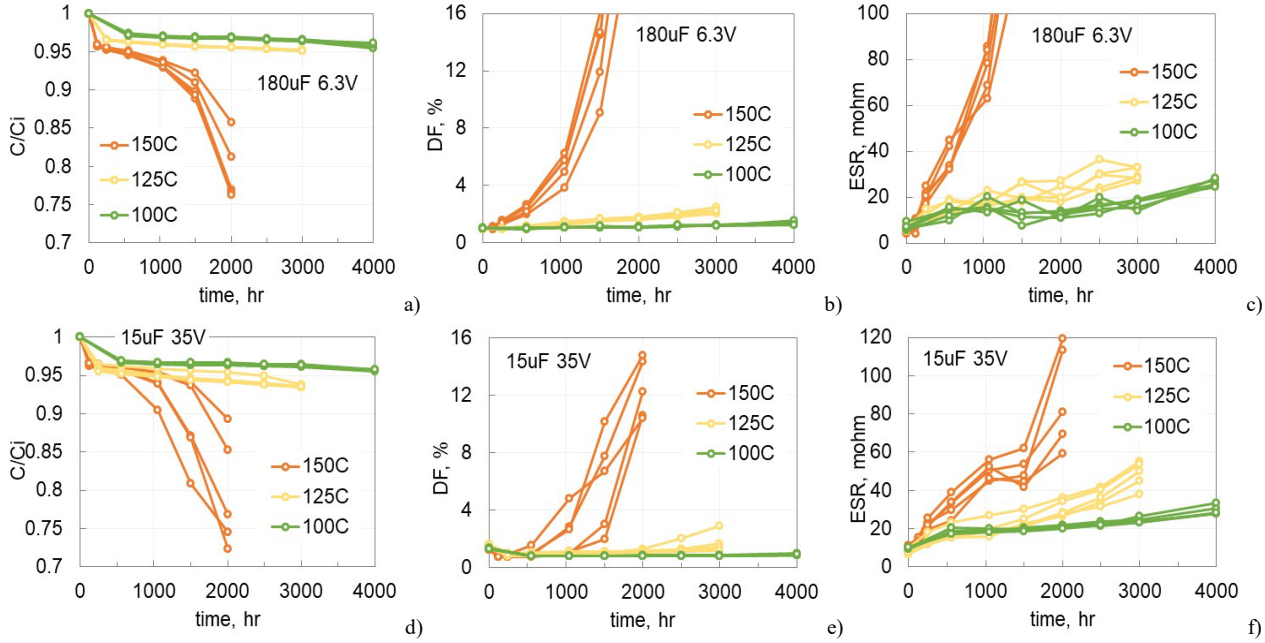

Fig. III.1. Variations of normalized capacitance (a, d), DF (b, e) and ESR (c, f) for 180 µF 6.3 V (a - c) and 15 µF 35 V (d - f) during HTS at three temperatures.

The parts are considered parametric failures if their capacitance decreased more than 10% of the initial value, or if DF increased more than 2 times of the initial limit (IL), or if ESR increased more than 3 times of the IL. The times to failure (TTF) were determined for each sample either directly from the curves similar to Fig.III.1 or by extrapolation of the data as shown in Fig.III.2a. Median times to failure calculated based on TTF distributions for capacitances and ESR are plotted in Arrhenius coordinates in Fig. III.2.b and c. Activation energies of the degradation varied from 0.64 to 0.9 eV for capacitance and in somewhat wider range, from 0.57 to 1.03 eV for ESR failures. However, the average activation energies were practically the same, $E_{a\_C} = 0.73 \pm 0.1$ eV, and $E_{a\_ESR} = 0.73 \pm 0.16$ eV. Extrapolation of the lines in Fig. III.2 to 65 °C that is assumed as the temperature of applications, resulted in the median TTF values from 6 to 48 years.

The values of E_a for PTCs were similar and also varied in a wide range, from 0.38 to 0.93 eV, averaging at 0.62 ±0.17 eV [17]. For both types of capacitors, the degradation was due to thermo-oxidative processes in conductive polymers and should be substantially less in vacuum compared to air environments. For this reason, successful results of qualification testing at 125 ºC for 1000 hours in air should guarantee long-term stability of characteristics at operating conditions in vacuum.

Another possible reason for APCs degradation during HTS is increasing of ESR due to changes in the hydrated layer of the Al2O3 dielectric. According to [2], water molecules trapped at the interfaces between the conductive polymer and oxide during manufacturing can form aluminum hydroxide that is conductive and might acts as an additional resistive layer in series with the conductive polymer. However, our data show that contrary to PTCs, where the rate of degradation of ESR is substantially greater than degradation of capacitance, the values of TTF_C and TTF_{ESR} for APCs are similar (see Fig. III.2 b, c). It is possible that the difference is due to a diffusion delay associated with penetration of oxygen inside the deep and narrow pores of aluminum oxide filled with conductive polymer compared to the sponge-like structure of

the pores covered with a relatively thin layer of conductive polymer in tantalum capacitors. This structure of pores in PTCs enhances diffusion processes and results in a faster degradation of ESR.

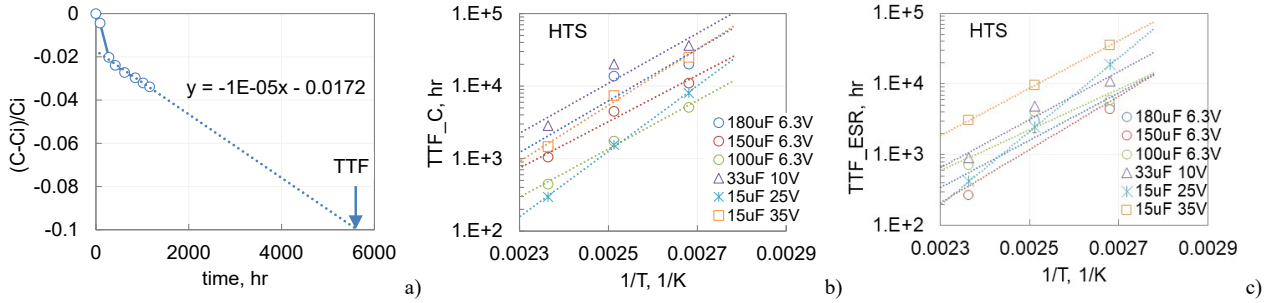

Fig. III.2. TTF calculation (a) and temperature dependencies of median times to parametric capacitance failures determined as a decrease by 10% compared to the initial value (b) and ESR failures (c) determined as a 3-time increase compared to the specified value.

HTS resulted in a substantial, up to three orders of magnitude, increase in currents after HTS at 150 °C for all part types (see Fig. III.3.a, b). At 125 °C, the increase was also noticeable, up to an order of magnitude, but storage at 100 °C for 4000 hours did not change currents significantly. The charts in Fig. III.3 also show variations of leakage currents after simulations by three reflow cycles at T_{max} = 235 °C for 4 types of APCs rated to 6.3 V. Due to a short duration of exposure to high temperatures, solder reflow did not cause significant variations in leakage currents.

A noticeable increase of DCL, up to two orders of magnitude, in wet tantalum and aluminum electrolytic capacitors after HTS was reported earlier [18]. It is possible that one of the reasons for DCL degradation in APCs is also due to the release of trapped electrons from deep states inside of Al2O3 dielectric that reduces the barrier at the interface oxide/conductive polymer and increases the Schottky conductivity through the dielectric. Another possible mechanism of increasing leakage currents is dissociation and out-diffusion of water molecules from the outer, hydrated layer of the aluminum oxide that can cause embrittlement of the layer and an increase in concentration of defects [19]. A substantial, about three orders of magnitude, increase in leakage currents after 2000 hours at 150 °C might be also due to mechanical damage in the deep pores in aluminum foil filled with polymer having a much larger coefficient of thermal expansion (CTE) compared to aluminum and Al2O3.

Breakdown voltages decreased after HTS for all part types except for 150 µF 6.3 V and 15 µF 25 V. Three cycles of reflow soldering resulted in approximately 10% reduction of breakdown voltages. Animalous charging currents, ACC, were not detected in any of the parts before or after HTS. As it will be shown in the next section, the presence of moisture increases breakdown voltages. Respectively, desorption of water molecules during HTS decreases VBR.

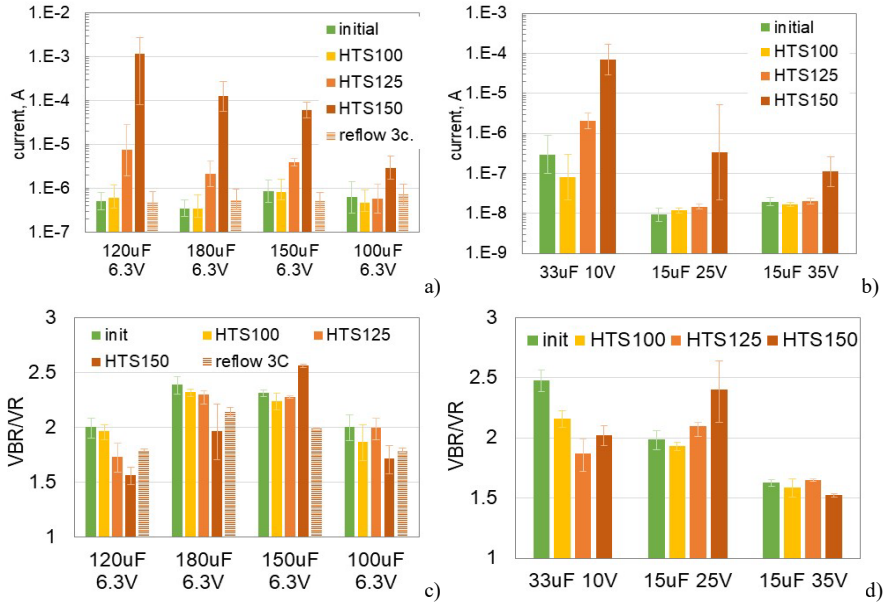

Fig. III.3. Effect of HTS on median values of DCL (a, b) and average values of breakdown voltages (c, d) for the seven types of APCs. Note that here and below, error bars indicate standard deviation of the relevant distributions.

IV. EFFECT OF HUMIDITY

The effect of storage in humid environments was evaluated at three conditions: (1) 20 °C, 95% RH for 1500 hr, (2) 85 °C, 60% RH for 500 hr, and (3) 85 °C, 85% RH for 850 hr. AC characteristics were measured periodically through the testing using five samples from each part type. Measurements of leakage currents and breakdown voltages were carried out after humidity testing.

Results of measurements of AC characteristics for capacitors from groups 5, 6, and 7 (refer to Table II.1) during storage at 20 °C and 95% RH are shown in Fig. IV.1. Most variations of capacitance and DF occur by 1000 hours of storage; but after, characteristics continued to change, but at a lower rate. The increase of capacitance after 1500 hours was ~ 5% for gr.5 and 7 and 17% for gr.6. Dissipation factors increased by a factor of 2-3 times, but remained within the specified limits. The most surprizing result of these tests was the stability and limited change in ESR (variations below 30%).

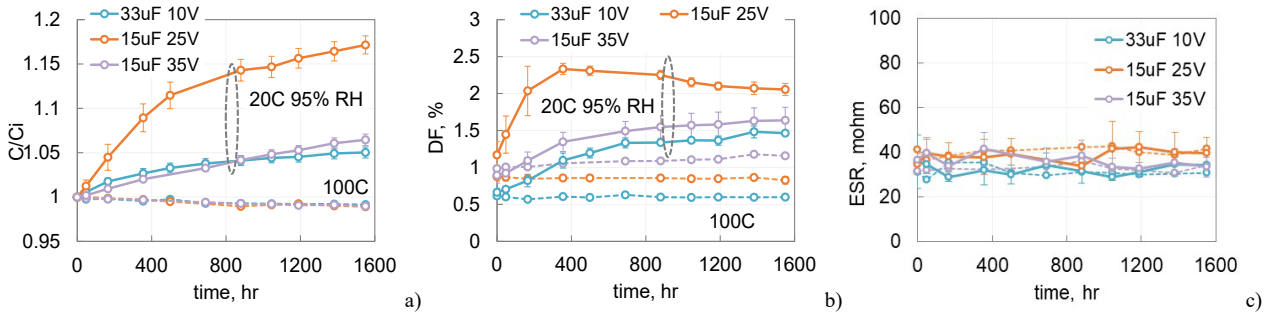

Fig. IV.1. Variations of normalized to the initial value capacitance (a), DF (b) and ESR (c) with time of storage at 20 °C and 95% RH (solid lines). As a reference, dashed lines show variations of characteristics during HTS at 100 °C (HTS100).

Measurements during storage at 85 °C and 60% RH (see Fig. IV.2) show that the increase of capacitance stabilizes by less than 200 hours at the levels that are 3% to 6% higher than the initial values. An increase in DF was less than 2.5 times, and most of the parts, had stable ESR values, except for gr.3 where ESR have risen by approximately 50%.

For most part types, variations of capacitance in the process of storage at 85 °C and 85% RH (see Fig. IV.3) stabilized also by 200 hours, but for gr.2 and especially for gr.3, capacitance did not stabilize even after 850 hours. By the end of the testing, the increase of capacitance varied from 5% in groups 1 and 4 to 35% in gr.3. Dissipation factors had a tendency of gradual increasing for all part types, but the increase was especially noticeable for gr.3 where DF at the end of testing exceeded the specified limit of 6% more than two times. The values of ESR remained stable for all parts, except for gr.3, where degradation started after 400 hours of storage, and by the end of the testing exceeded the specified limit more than ten times.

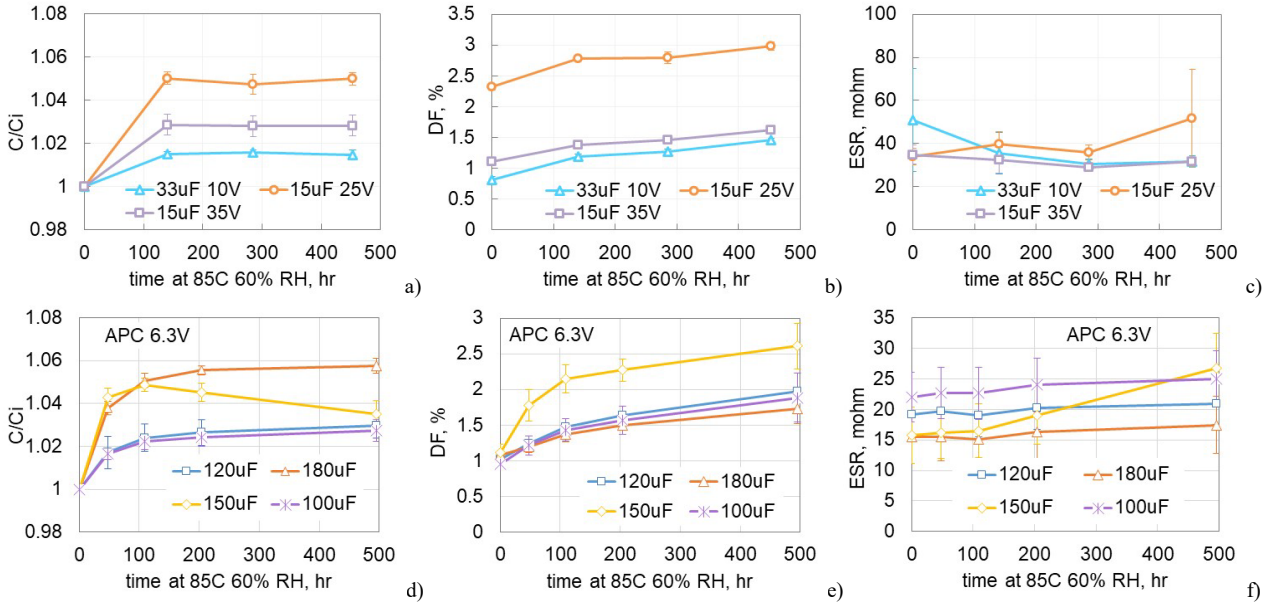

Fig. IV.2. Variations of normalized capacitance (a, d), DF (b, e) and ESR (c, f) with time of storage at 85 °C and 60% RH for capacitors rated to 10 V and above (a-c) and for 6.3 V capacitors (d-f).

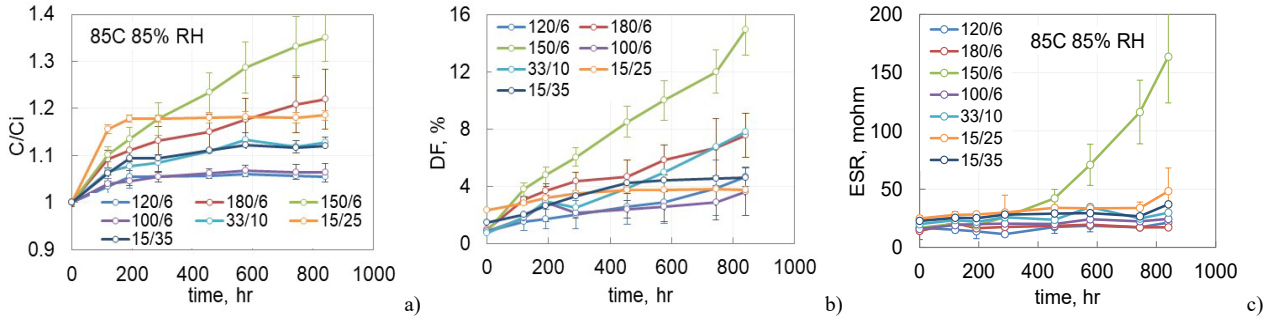

Fig. IV.3. AC characteristics for the seven types of capacitors in the process of storage at 85 °C and 85% RH. The legends indicate values of capacitors in μF and rated voltages in volts.

Variations of capacitance for APCs were similar to what was observed for PTCs [20] but degradation of DF was larger, likely due to the presence of the outer hydrated oxide layer in aluminum electrolytic capacitors. This layer can be easily polarized and generate relatively large losses [19]. Apparently, additional hydration caused by exposure to high temperature and high humidity can result in degraded DF values.

Results of post humidity storage measurements of operational leakage currents (currents measured after 1000 sec of electrificationa) and breakdown voltages normalized to the rated voltage are shown in Fig. IV.4. For comparison, breakdown voltages measured for dry capacitors (after 100 hours of HTS100) and capacitors after long (more than 3 month) storage at room conditions (RC) are also shown.

For all part types, except for gr.1 and gr.4, leakage currents increased approximately two orders of magnitude after storage at 85 °C and 85% RH. Note, that these two groups had no significant changes in leakage currents after storage at 60% RH and had also more stable AC characteristics. All parts after storage at 85 °C and 60% RH had leakage currents within the specified limits. Degradation of AC and DC characteristics caused by moisture sorption apparently does not depends on the thickness of the plastic packages. The rate and degree of degradation for gr.2 and gr.7 that had H = 2.8 mm was not less than for the rest of the parts having H = 1.9 mm.

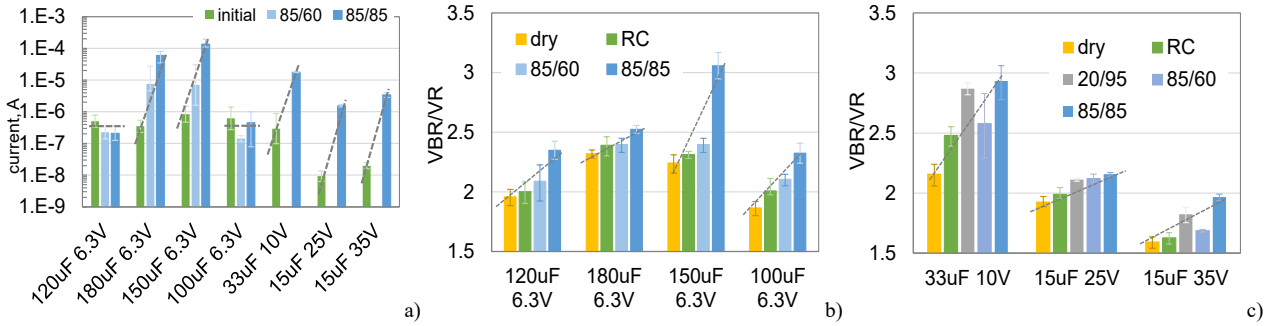

Fig. IV.4. Effect of storage in humidity chambers on median values of leakage currents (a) and average values of the normalized breakdown voltages (b, c).

The behavior of leakage currents in APCs was different from TPCs, where currents reduced in the presence of moisture due to the suppression of anomalous transients and remained stable up to 1000 hours of storage at 85 °C 85% RH. However, the effect of moisture on breakdown voltages was similar. The presence of moisture increased VBR in different APCs by 10 to 36% (see Fig.IV.4.b and c). On average, the increase of VBR after storage at 85 °C and 85% RH was 23 ±10%. This is similar to what was observed in PTCs [21] where breakdown voltages for 14 lots of capacitors increased by 21 ±14%. For PTCs this effect was explained by reduction of leakage currents, but for APCs that did not have anomalous transients, the prevailing mechanism is different. For APCs the effect is likely due to additional anodic oxidation of the defective areas in the dielectric in the presence of moisture and high electric fields that results in effective self-healing of the parts before breakdown.

Relaxation of leakage currents in capacitors rated to 6.3 V measured initially, after storage at 85 °C and 85% RH and after 1000-hour testing at 20 °C and 9 V are shown in Fig. IV.5. After saturation with moisture, leakage currents in gr.2 and gr.3 capacitors increased substantially (~ two orders of magnitude), but decreaed with time under bias. This decrease is especially noticeable during 1000 hr testing at 9 V. After approximately an hour, currents in these groups started decreasing gradually, roughly inversely proportional with time, and by 1000 hours reduced to almost three orders of

magnitude. The post stress leakage currents at 6.3 V were about an order of magnitude smaller than initially (compare Fig. IV.5.a and d).

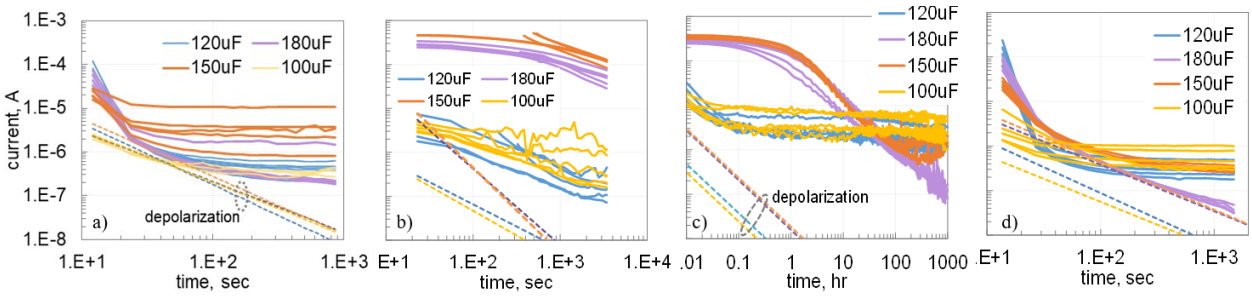

Fig. IV.5. Leakage currents in APCs rated to 6.3 V initially (a), after humidity chamber at 85 °C 85% RH for 850 hr (b), during post-humidity 1000-hour stress test at 9 V (c), and after stress testing (d). Dashed lines correspond to absorption currents in the parts measured during tepolarization.

Additional tests showed that the moisture diffusion delay in the parts at room conditions is more than 10 hours, and noticeable changes caused by moisture desorption start after ~ 30 hours. This means that the observed decrease in leakage currents can not be explained by moisture outdiffusion only. It is possible that additional anodic oxidation in the presence of moisture self-healed defects in the oxide and reduced leakage currents. Another possible mechanism is electron trapping in deep states of the oxide or in conductive polymer that increased the Schottky barrier and reduced conduction in the capacitors. Apparently, manufacturing conditions during oxide and conductive polymer formations in groups 2 and 3 capacitors were different compared to groups 1 and 4. This is also confirmed by variation of absorption (depolarization) currents. Initially, these currents were similar in all four types of capacitors; however, after storage in humidity chamber, absorption currents for groups 2 and 3 were almost an order of magnitude greater indicating an increased concentration of traps in these parts [20]. It is also possible that the presence of moisture intensifies processes of uptake and release of ionic charges in the bulk of conductive polymers that contribute to the absorption capacitance and currents in the system [22].

V. HIGHLY ACCELERATED LIFE TESTING

HALT for capacitors rated to 6.3 V was carried out using 20 smaples in each group. All parts were reflow soldered onto test boards and each capacitor was connected in series with a 62 mA fast acting fuse. Voltage drops across the fuses were monitored by scanning voltages across the fuses that had 7 ohm resistance alowing for assessments of the leakage currents and determining times of failure by open fuses. First, the testing was carried out at 85 °C and 9 V (1.43VR) for 1000 hours. As a result of these tests (see Fig. V.1) two samples failed in group 1 and 3 samples failed in group 4. Three samples in group 2 had significant current spikes reaching hundreds of microamperes, indicating powerful scintillation events. Group 3 capacitors did not have failures or scintillations, but initially, the currents increased gradually for a few hours reaching hundreds of microamperes, then decreased slowly to the level of a few microampers after 400 hours.

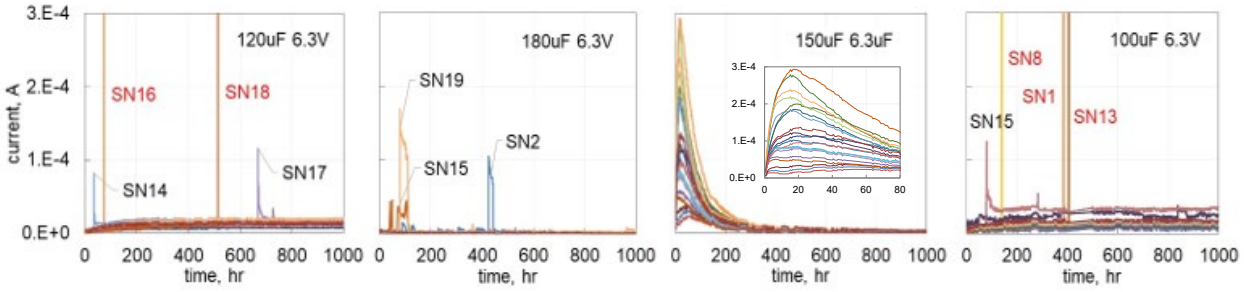

Fig. V.1. Monitored leakage currtents during HALT at 85 °C and 1.43VR for four groups of APCs rated to 6.3 V. Serial numbers in red font indicate failures caused by blown fuses and in black font to scintillation events.

Results of post-HALT measurements of AC characteristics and leakage currents are shown in Fig. V.2. Median values of capacitance decreased by 9% in group 2 and 3 and only by 1 to 2% for capacitors in group 1 and 4. These results are likely due to moisture desorption during HALT. Median values of DF increased more significantly, by 67% and 57% for groups 1 and 4, and approximately two times in groups 2 and 3. Median values of ESR increased substantially, in 10 to 15 times, for all groups. Note, that approximately 20% of the parts had initial ESR values outside the specified limits.

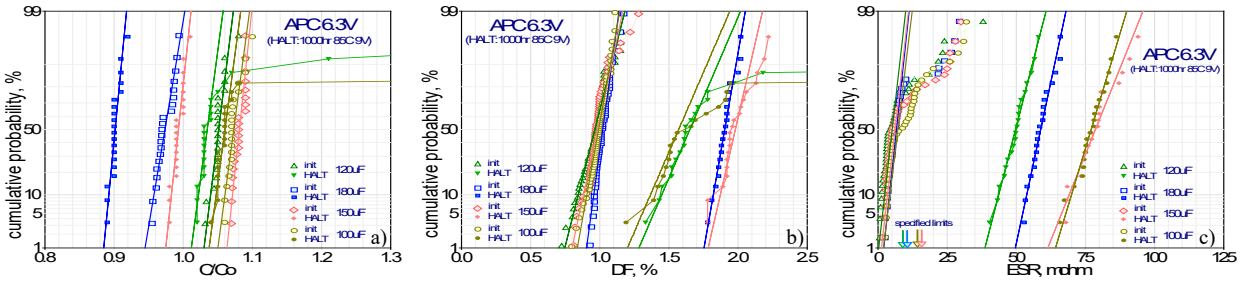

Fig. V.2. Effect of a 1000-hour HALT at 85 °C and 9 V (1.43VR) on capacitance (a), DF (b), and ESR (c) for APCs rated to 6.3 V.

After 1000 hours at 85 °C and 9 V all samples in groups 2 and 3 had acceptable characteristics, and only 10% of samples in group 1 and 15% in group 4 failed. Samples that remained functional after 9 V HALT were used for additional stress testing at 85 °C and 11 V (1.75VR) for 710 hours. At these conditions, all samples in groups 1 and 4 failed within one hour of testing. Variations of leakage currents during 11 V HALT for groups 2 and 3 are shown in Fig. V.3. Leakage currents in group 2 capacitors were unstable, but decreased with time and stabilized after ~200 hours. Six out of 20 samples failed within first 24 hours of testing, but no more failures were detected for the next 690 hours. Two out of six failed samples were the parts that exhibited scintillation events during 9 V HALT, and for this reason powerful scintillations can be considered as failures. Leakage currents in group 3 capacitors increased with time with a hump after a few hours of testing, but no current spiking or failures were observed. The presence of humps in these parts might be associated with additional oxide formation that was observed also in wet aluminum electrolytic capacitors [23].

Distributions of resistances measured after 11 V HALT (Fig.V.3.c) show that all samples in groups 1 and 4 failed short circuit with a median resistance of less than 20 ohms, whereas 40% of group 2 and all parts in group 3 had resistances exceeding 10 Mohm. After HALT, capacitance in group 3 decreased by 17% compared to the initial values, DF increased by 83%, and ESR increased approximately tenfold. Leakage currents post HALT at 9 and 11 V had a tendency of increasing with the higher stress voltage in groups 1 and 4 and decreasing for groups 2 and 3 (see Fig.V.3.d). This is likely due to the differences in manufacturing processes, e.g. oxide formation, or cathode materials used.

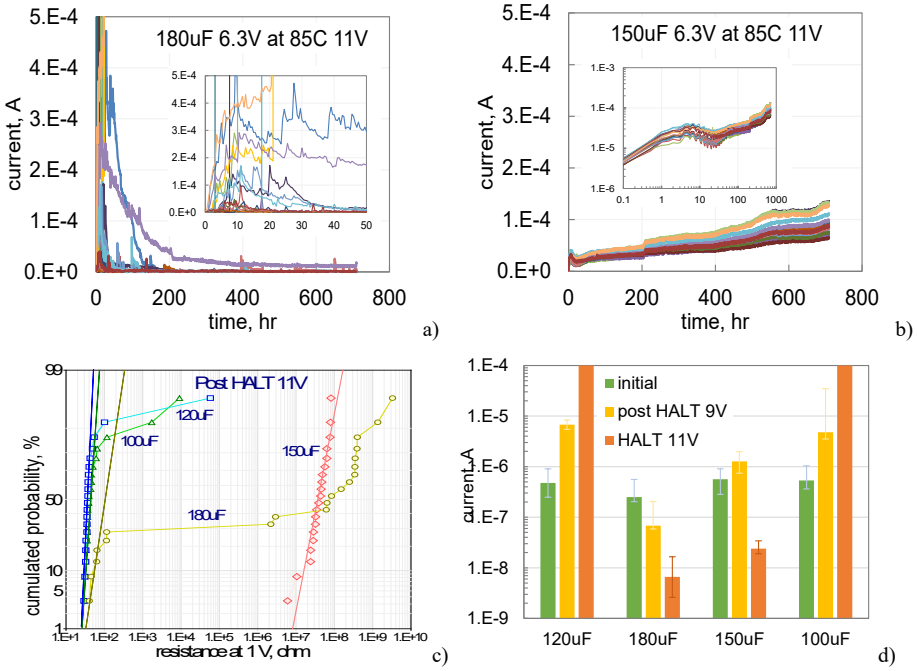

Fig. V.3. Leakage currents during HALT at 85 °C and 1.75VR for gr.2 (a) and gr.3 (b) capacitors. Figure (c) shows distributions of resistances after HALT at 11 V and figure (d) illustrates variations of leakage currents after different HALT conditions. Insets in figures (a) and (b) show the same I-t curves in different scales.

Due to a wide range of TTF for different groups of capacitors, HALT-2 was carried out at 85 °C and 10 V for groups 1 and 4, and at 12 V for groups 2 and 3 capacitors. Results of these tests are shown in Fig. V.4. Most failures (90%) in group 1 (120 µF) occurred by 100 hours and in group 4 (100 µF) by 30 hours of testing. Results for group 2 (180 µF)

were similar to HALT at 11 V: majority of the parts (70%) failed by 1 hour, and all capacitors, except for one sample that remained functional through the testing, failed by 7 hours. TTF distributions in Weibull coordinates for groups 1 and 4 capacitors were bymodal indicating the presence of infant mortalty (IM) and WO failures. All groups had samples deviating from WO distributions to longer times forming a group of so-called anti-WO failures. No failures were observed in capacitors from group 3 (150 µF), but leakage currents in these parts had spikes as shown in Fig. V.4.b. Post-HALT-2 measurements of resistances (see Fig. V.4.c) indicate that approximately half of samples from groups 1 and 4 and 90% of samples from group 2 failed hard short circuit with resistances below 100 ohm. The rest of parts had resistances in the kohm range. This indicates that some samples can decrease leakage currents even after powrfull scintillations causing opened 62 mA fuses. Group 3 capacitors that did not have failures had leakage currents in the microampere range, and respectively, their resistances were in the megaohm range.

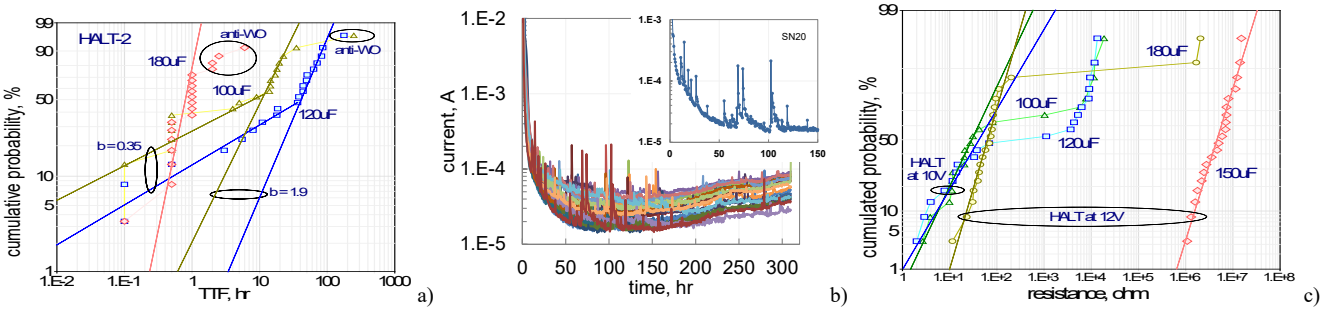

Fig. V.4. Distributions of times to failure during HALT-2 (a), variations of leakage currents for gr.3 (150 µF) capacitors (b), and distribution of resistances measured after HALT-2 (c). Inset in Fig.(b) shows an example of spiking in SN20. Note that actual values of maximum currents during spikes are likely much higher than the ones detected during scanning every 15 min.

Capacitance values after HALT-2 decreased on average by 15% and 25% in groups 2 and 3, whereas capacitance for half of the samples in groups 1 and 4 remained stable, but incresed up to 3.5 times for the rest of the samples. Increased capacitance values were expected for samples with low resistances. Dissipation factor in group 1 and 4 capacitors increased from 10 to 100 times. For half of the group 2 samples, the DF increase was ~20 times, but for group 3 capacitors DF had risen by only 50%. The values of ESR increased in all parts between 10 to 20 times. Results show that the most sensitive to degradation parameters are DF and ESR, and in many cases resulted in parametric failures of the parts.

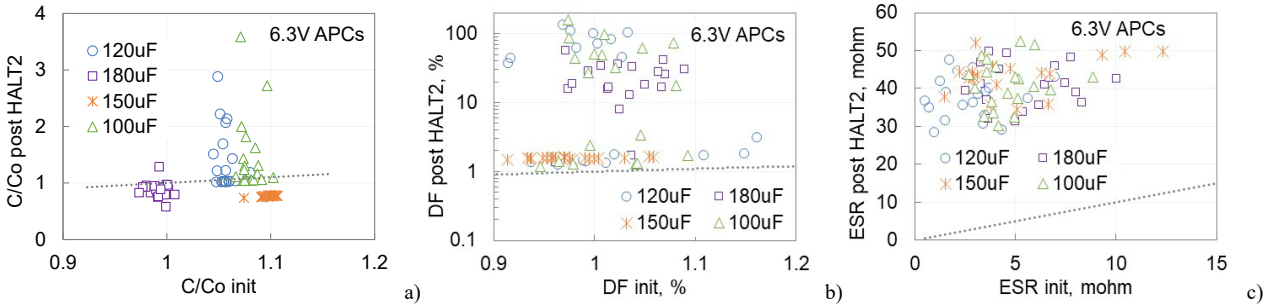

Fig. V.5. Correlation of AC characteristics measured before and after HALT-2. Dotted lines correspond to no change values.

Considering that the level of stress during HALT-2 was excessive for all part types except for gr.3, HALT-3 was carried out at 85 °C and 9.5 V (1.51VR) for 120 µF and 100 µF capacitors and at 11.5 V (1.83VR) for 180 µF and 150 µF capacitors. Similar to the previous HALT conditions, most failures in group 2 parts (~80%) occurred early, by 2 hours of testing, but the remaining 4 samples remained operational till the end of test at 1100 hours (Fig. V.6.a). Except for the first two initial failures, majority of the parts follow Weibull distribution with the slope 1.6 indicating WO failures. Respectively, the remaining 4 samples that did not fail after 1100 hours belong to the anti-WO group. The currents in these samples, although unstable and exhibiting scintillation breakdowns, gradually decreased with time (see Fig.V.6.b).

Group 3 samples (150 µF) as in the previous case, had no failures and the current spikes were much less substantial compared to HALT-2 and to group 2 capacitors during HALT-3 (Fig.V.6.b). This indicates a strong dependence of the probability of scintillations on the voltage stess. Median times to failure during HALT-3 at 9.5 V were 430 and 150 hours respectively for 120 µF and 100 µF capacitors. In some cases, failures occurred after powerfull scintillation events with currents recovering after dozens of hours of testing (see SN20 of 120 µF and SN14 of 100 µF capacitors in Fig. V.6.c).

However, similar events might not result in short circuit failures even after several scintillations as shown for SN14 of 120 µF APCs.

After HALT-3, leakage currents were monitored at rated voltage and 20 °C for one hour. The currents increased in different groups from 10 to 30 times compared to the initial values, but no spiking was observed.

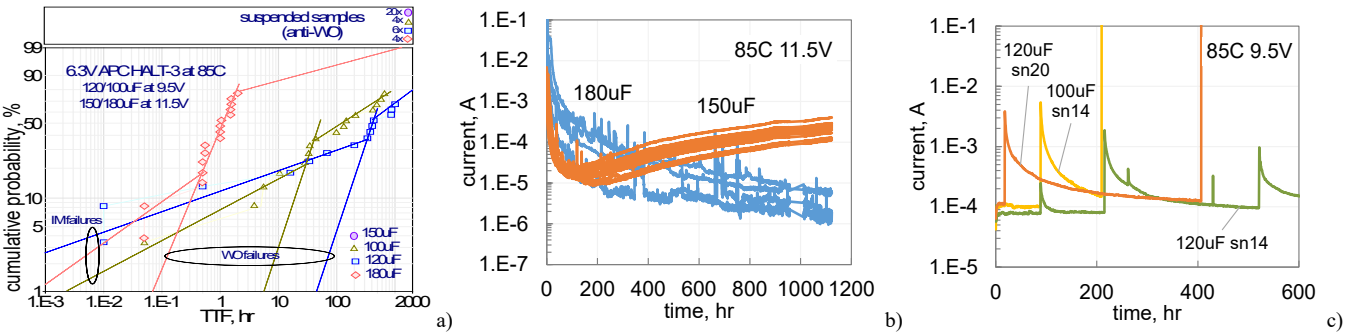

Fig. V.6. Distributions of times-to-failure for three part types (a), leakage currents measured during HALT-3 at 85 °C and 11.5 V for gr.2 and 3 capacitors (b), and examples of scintillation current spikes in gr. 1 and 4 capacitors tested at 9.5 V and 85 °C (c).

To get a better understanding of the behavior of APCs during HALT, currents in all 7 groups of capacitors were monitored for 1000 hours at 125 °C using 10k current sense resistors instead of fuses. Five samples in each group of capacitors rated to 6.3 V and 15 samples for capacitors rated to higher voltages (groups 5, 6, and 7) were used for this study. Capacitors rated to 6.3 V were tested at 9 V (1.43VR), capacitors rated to 10 V were tested at 1.4VR, and capacitors rated to 25 and 35 V were tested at 1.2VR.

Results of 125 °C testing for 6.3 V capacitors are displayed in Fig. V.7. No short circuit failures were detected in any of the groups; however, all parts, except for group 3 (150 µF) exhibited current spikes. During scintillation events, the currents increased sharply typically by 1 to 3 orders of magnitude, and then decreased gradually, for hours, to the initial level. Considering that the proportion of samples during HALT at 85 °C and 9 V was ~15% only (see Fig.V.1), rising temperature during HALT increases the probability of scintillations.

Capacitance after HALT at 125 °C decreased by 3 to 7% in all groups except for groups 2 and 3 where the decrease was ~20%; DF increased by 20 to 70% in all groups except for groups 1 and 4, where the rise was 5 and 12 times, and group 5 where DF decreased ~50%. The values of ESR increased on average from 5 to 7 times in all types of capacitors except for group 5 (33 µF 10 V) where the increase was relatively small, ~10%.

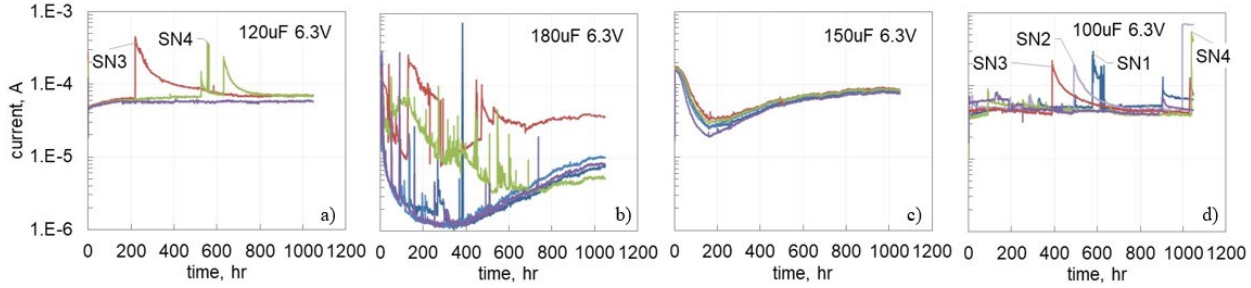

Fig. V.7. Leakage currents in APCs rated to 6.3 V during HALT at 125 °C and 1.43VR.

Leakage spikes were also observed in capacitors rated to 10 V and above (Fig.V.8). The spiking started after a certain incubation period (typically after more than a dozen of hours) that is required to accumulate defects in the dielectric before scintillation breakdowns occur. In all cases, similar to 6.3 V capacitors, the currents increased sharply by orders of magnitude and then gradually, within hours, relaxed to the initial or some times higher levels. A similar behavior was also observed in PTCs, but in many cases in tantalum capacitors the spiking was due to gradual increasing of currents and followed by a sharp decrease to the initial levels [24]. A sharp increase is due to a short duration of scintillation events that, based on oscilloscopic measurements during CCS testing, occurs within milliseconds. The termination of scintillations is due to self-healing processes that may take hours to complete.

A commonly used self-healing model that assumes a conversion of conductive polymers into high resistive state, caused by local overheating during scintillation to above 300 °C [1, 2, 25], cannot explain this behavior. It is possible that similar

to what was suggested for PTCs, local overheating during scintillations changes the distribution of charges trapped in deep states of the dielectric or dielectric/conductive polymer interface, thus subtantially reducing the barrier for the charge flow [15]. Over time, the current refills empty states, increases the barrier, and reduces the leakage.

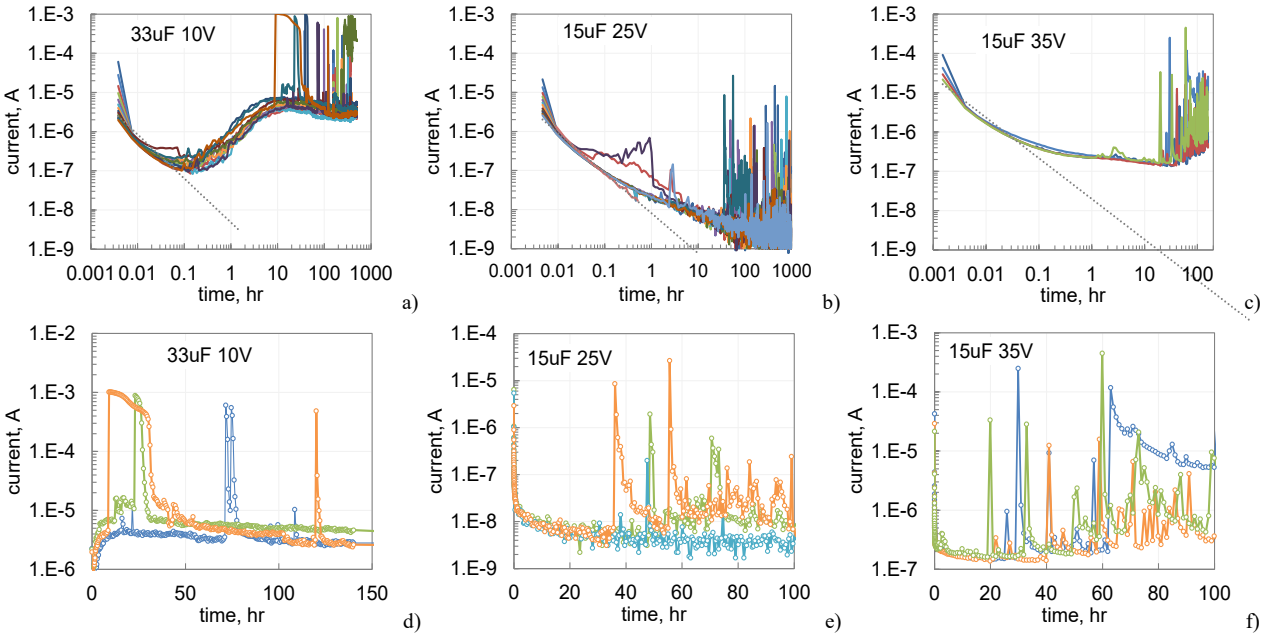

Fig. V.8. Leakage currents in different types of APCs during HALT at 125 °C. Capacitors rated to 10 V (a) were stressed at 1.4VR, and capacitors rated to 25 V (b) and 35 V (c) at 1.2VR. Figures (d – f) show examples of current spikes observed during the testing.

Samples that passed HALT were tested for breakdown voltages using a CCS technique. Average normalized values of VBR are compared with the values for dry, virgin samples (initial) in Fig. V.9 and indicate increasing VBR caused by HALT. Note that the observed rise of VBR (up to 30%) substantially exceeds the coefficient of variations (below 5%) and cannot be explained by survival of parts that had initial higher levels of VBR. This rise is likely due to additional anodic oxidation caused by water molecules remaining in the system even after prolonged operation at 85 °C and may explain the anti-WO phenomena.

The characteristic times to WO failures are plotted against stress voltages during HALT in Fig. V.9.b. The values of normalized breakdown voltages were also used assuming TTF of ~ 10 sec, which is an average duration of CCS testing. In semi-logarithmic coordinates, the data can be linearized indicating an exponential dependence of $TTF_c(V)$ that can be derived from the thermochemical time dependent dielectric breakdown (TDDB) model [26]:

$$TTF_c(V) = t_0 \times \exp\left(-B\frac{V}{VR}\right) \quad ,$$

where t_0 and B are constants.

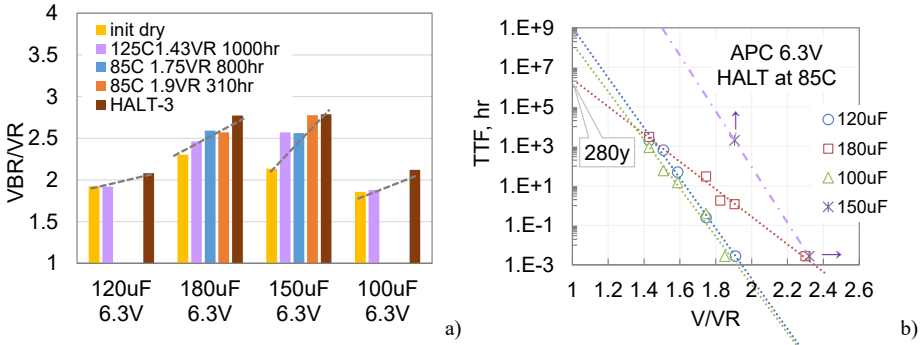

Fig. V.9. Variations of the normalized breakdown voltages after different HALT conditions (a) and voltage dependence of the characteristic times to failure (b).

The values of voltage acceleration constant B for parts shown in Fig. V.9.b vary from 16 for 180 µF to 29 for 120 µF capacitors, which are substantially greater than for PTCs [27]. Extrapolations to the rated voltage indicate that the characteristic times of WO failures at 85 °C exceed 280 years. Assuming that the time to inception of WO failures, (TTF_i)

or useful life of the parts, corresponds to the probability of failure of 0.1 %, this time can be calculated based on the characteristic *TTF* and the slope of Weibull distributions (β):

$$TTF_i(VR) = TTF_c(VR) \times [-\ln(0.999)]^{1/\beta} \ ,$$

Considering that the slopes are in the range from 1.6 to 2.8, the useful life of the parts exceeds 3 years of operation at 85 °C and at 6.3V. However, voltage derating to 4 V will make this time practically endless, more than 5,000 years.

VI. SUMMARY

Analysis of the performance of 7 types of aluminum polymer capacitors with rated voltages from 6.3 to 35 V, encapsulated in plastic cases with the same footprint EIA 7343, and manufactured by four different vendors showed that their behavior and reliability differ substantially. Assuring proper storage, handling, screening, lot acceptance testing, and derating, some types of APCs can be used in spaceflight applications.

1) Behavior of the parts during high temperature storage is similar to polymer tantalum capacitors, PTCs, and results in decrease of capacitance and increase of DF and ESR.
   a) All part types failed ESR after a few hundreds of hours at 150 °C, but no parametric failures (increase above 3 times of the specified value) were detected after 1000-hour storage at 125 °C.
   b) Storage at temperatures exceeding 100 °C resulted in increased DCL, approximately an order of magnitude after 3000 hours at 125 °C and up to 3 orders of magnitude after 2000 hours at 150 °C. However, the currents remained within the specified limit after 4000 hours of storage at 100 °C.
   c) Breakdown voltages reduced by 2 to 12% after HTS100 for all part types, and by 3 to 25% after HTS125 for 5 out of 7 types of capacitors.
   d) Three cycles of reflow soldering at T_{max}= 235 °C did not degrade leakage currents but reduced breakdown voltages by ~10% in capacitors rated to 6.3V.
   e) Contrary to PTCs, no anomalous charging currents (ACC) were observed in any of the tested APCs initially or after HTS.
   f) Activation energy of HTS failures calculated based on capacitance or ESR degradation is 0.73 ±0.16 eV, which is close to the PTC values. Extrapolations of times to failure observed in the range from 100 to 150 °C to operating conditions (65 °C) indicate TTF in the range from 6 to 48 years. Similar to PTCs, successful testing in air at 125 °C for 1000 hours will assure significantly longer (more than 20 years) operational times in vacuum.

2) Storage in humid environments at 85% RH and 85 °C for 850 hours resulted in parametric failures for 2 out of 7 part types, but no significant degradation or failures were detected during storage at 85 °C and 60% RH for 560 hours. The latter condition may be sufficient to assure reliable applications of APCs during terrestrial testing and integration periods.
   a) After storage at 85 °C and 85% RH, different types of APCs increased capacitance by 5 to 35%, DF in 2 to 15 times, but there were no significant changes of ESR for all parts except for 150 μF 6.3 V capacitors where ESR increased more than 8 times.
   b) Contrary to PTCs, where leakage currents reduce in the presence of moisture due to suppressed anomalous transients, leakage currents in APCs increased up to 100 times after storage at 85 °C and 85% RH for 5 out of 7 part types, but less than 10 times after storage at 85 °C and 60% RH. The excessive leakage currents after storage in humid environments decrease gradually with time under bias to the levels lower than the initial currents.
   c) Breakdown voltages increased in the presence of moisture in all tested types of APCs from 8 to 35% after storage at 85% RH and from 3 to 19% after storage at 60% RH. This increase was likely due to additional anodic oxidation in the process of breakdown measurements.

3) Monitored HALT at 85 °C and voltages ranging from 1.4VR to 1.9VR showed that reliability of different types of capacitors rated to 6.3 V varied from 90% of samples failing before 30 hours at 10 V in 100 μF capacitors to no failures after 1100 hours at 11.5 V for 150 μF parts.
   a) Similar to tantalum, APCs have infant mortality, wear-out, and anti-WO failures. The latter is due to increasing of breakdown voltages (from 8 to 30% for different part types) during HALT. The presence of IM failures indicates the need for burn-in screening.
   b) Dependence of the characteristic times-to-failure on stress voltage can be described using an exponential thermochemical TDDB model with high voltage acceleration constants *B* (from 16 to 29 for different part types), which is substantially greater than for TPCs.

c) Estimated TTF_c values at 85 °C and VR exceed 280 years and useful life determined at 0.1% of wear-out failures at 85 °C and voltages derated to below 65% VR would exceed thousands of years.
d) The intensity of current spikes during HALT caused by scintillation breakdowns increases with time, temperature, and the level of voltage stress. Group 3 capacitors (150 µF 6.3V) had no failures at all used HALT conditions and contrary to other types, had minimal or no current spiking indicating that APCs can be used reliably in space applications.

VII. ACKNOWLEDGMENT

The author is thankful to Chris Tiu, NASA GSFC Code 562 Associate Branch Head for his review and discussion and to Peter Majewicz, NASA NEPP Program Manager, for his support on this study. This work could not have been done without help of the GSFC Parts Analysis Lab specialists.

VIII. REFERENCES

[1] J. D. Prymak, "Improvements with polymer cathodes in aluminum and tantalum capacitors," in *APEC 2001. Sixteenth Annual IEEE Applied Power Electronics Conference and Exposition (Cat. No.01CH37181)*, 2001, 4-8 March 2001, pp. 1210-1218 vol.2.
[2] L. L. Macomber, "Solid polymer aluminum capacitor chips in DC-DC converter modules reduce cost and size and improve high-frequency performace," presented at the PCIM Power Electronics 2001, Rosemont, IL, 2001. https://www.cde.com/resources/technical-papers/spa2.pdf
[3] Murata. (2022). *Polymer Aluminum Electrolytic Capacitors*. Available: https://www.murata.com/en-us/products/capacitor/polymer
[4] V. B. Steffen Buhrkal-Donau, Thomas Ebel, "A way to High Voltage Polymer Aluminium Electrolytic Capacitor," presented at the PCNS'21, Milan, It, 2021.
[5] S. Neupane, O. E. Olawale, V. Adashkevich*, et al.*, "Long-term testing results of a high-performance 450 V Polymer Aluminum Electrolytic Capacitor," in *2023 25th European Conference on Power Electronics and Applications (EPE'23 ECCE Europe)*, 2023, 4-8 Sept. 2023, pp. 1-6.
[6] Panasonic. (2022). *SP-CAP™ POLYMER ALUMINUM*. Available: https://na.industrial.panasonic.com/products/capacitors/polymer-capacitors/lineup/sp-cap-polymer-aluminum
[7] KEMET. (2023). *KEMET A798 Plus Performance Aluminum Organic Capacitor AO-CAP®*. Available: https://www.kemet.com/en/us/technical-resources/kemet-a798-plus-performance.html
[8] U. Merker, "Reaching the Next Level of Reliability for Polymer Capacitors," presented at the PCNS'21, Milan, It, 2021.
[9] F. PUHANE. (2020). *ANP071: Aluminum Electrolytic vs. Aluminum Polymer Capacitor*. Available: https://community.element14.com/products/manufacturers/wuerth-elektronik/w/documents/3740/anp071-aluminum-electrolytic-vs-aluminum-polymer-capacitor
[10] Panasonic_Reliability. (2022). *Safety and Legal Matters to Be Observed*. Available: https://api.pim.na.industrial.panasonic.com/file_stream/main/fileversion/2464
[11] A. Shrivastava, M. H. Azarian and M. Pecht, "Rapid Assessment Testing of Polymer Aluminum Electrolytic Capacitors in Elevated Temperature–Humidity Environments," *Journal of Failure Analysis and Prevention,* vol. 16, pp. 1059-1066, 2016/12/01 2016 https://doi.org/10.1007/s11668-016-0184-0
[12] J. Romero, M. H. Azarian and M. Pecht, "Reliability analysis of multilayer polymer aluminum electrolytic capacitors," *Microelectronics Reliability,* vol. 112, p. 113725, 2020/09/01/ 2020 https://www.sciencedirect.com/science/article/pii/S0026271419311266
[13] D. Liu, "NEPP report: Physical and Electrical Characterization of Aluminum Polymer Capacitors," 2009, https://nepp.nasa.gov/files/20389/09_005_GSFC_Williams_Liu%20APC%20Final%20Report.pdf
[14] A. Teverovsky, "Guidelines for Screening, Lot Acceptance, and Derating for Polymer Tantalum Capacitors," NASA STI Program, Greenbelt, MD, NEPP report 2023, https://ntrs.nasa.gov/api/citations/20220019033/downloads/20220019033-Teverovsky-2023-NASA-TP-Guidelines-Screening-PTC_v3.pdf
[15] A. Teverovsky, "Breakdown and Self-healing in Tantalum Capacitors," *IEEE Transactions on Dielectrics and Electrical Insulation,* vol. 28, pp. 663-671, 2021
[16] A.Teverovsky, "Metrics for Anomalous Charging currents in Polymer Tantalum Capacitors," in *2023 IEEE Electrical Insulation Conference (IEC)* Quebec City, Quebec, Canada, 2023, 18 June - 21 June 2023, pp. 169-173.
[17] A. Teverovsky, "Effect of High Temperature Storage on AC Characteristics of Polymer Tantalum Capacitors," in *International Conference on High Temperature Electronics (HiTec - iMAPS)*, virtual, 2021, April 26-29.
[18] A. Teverovsky, "Degradation of Aluminum and Tantalum Wet Electrolytic Capacitors during High Temperature Storage," in *4th PCNS Passive Components Networking Symposium*, Sønderborg, Denmark, 2023, September 11-13, pp. 129-140.
[19] K. Iida. (2023). *Essential Characteristics of Capacitors. DC leakage current.* Available: https://www.aictech-inc.com/en/valuable-articles/capacitor_foundation05.html
[20] A. Teverovsky, "Effect of Moisture on AC Characteristics of Chip Polymer Tantalum Capacitors," *IEEE Transactions on Components, Packaging and Manufacturing Technology,* vol. 9, pp. 2282-2289, 2019

[21] A. Teverovsky, "Breakdown and Self-healing in MnO2 and Polymer TantalumCapacitors," NASA STI Program, Greenbelt, MD, NEPP report 2021, https://nepp.nasa.gov/docs/tasks/003-Evaluation-Polymer-Tantalum-Capacitors-for-Space-Applications/2020-NASA-TM-Teverovsky-MnO2-Polymer-Tantalum-Capacitors-20205011704.pdf
[22] E. P. W. Jenkins, S. T. Keene, I. B. Dimov*, et al.*, "High capacitance freestanding PEDOT:PSS electrodes for low-frequency electric field delivery," *AIP Advances,* vol. 14, 2024 https://doi.org/10.1063/5.0180487
[23] A. Teverovsky, "Updates on Capacitors' Tasks," in *2023 Annual Electronic Technology Workshop, NEPP ETW*, Greenbelt, MD, 2023, June 12-15. https://nepp.nasa.gov/docs/etw/2023/14-JUN-WED/1610_Teverovsky_20230008485.pdf
[24] A. Teverovsky, "Evaluation of 10V chip polymer tantalum capacitors for space applications," presented at the ESA 2nd International Symposium - Space Passive Component Days, Noordwijk, The Netherlands, 2016.
[25] Panasonic, "Understanding polymer and hybrid capacitors," *White paper,* 2015 https://www.ttieurope.com/content/dam/tti-europe/manufacturers/panasonic/resources/Whitepaper_PolymerCapacitor.pdf
[26] A. Teverovsky, "Infant Mortality and Wear-Out Failures in Polymer and MnO2 Tantalum Capacitors," in *2022 IEEE International Reliability Physics Symposium (IRPS)*, 2022, 27-31 March 2022, pp. P46-1-P46-9.
[27] A. Eidelman, S. Zlatopolsky and A. Teverovsky, "Acceleration Factors for Reliability Assessment of Polymer Tantalum Capacitors," in *3rd PCNS Passive Components Networking Symposium*, Milan, Italy, 2021, September 7-10, pp. 119-129.